Stability analysis of a thick piezoelectric FGM plate

K. M. Bajoria & P. Jadhav
Department of Civil Engineering,
Indian Institute of Technology Bombay, India

Abstract

This paper investigates the stability analysis of plates made of functionally graded material (FGM) and subjected to electro-mechanical loading. A thick square FGM plate with piezoelectric actuator and sensor at top and bottom face is considered. The material properties are assumed to be graded along the thickness direction according to simple power-law distribution in terms of the volume fraction of the constituents, while the Poisson's ratio is assumed to be constant. The plate is simply supported at all edges. Using first order (FOST) and higher order shear deformation theories (HOST12), the finite element model is derived with von-Karman hypothesis and as a degenerated shell element. The displacement component of the present model is expanded in Taylor's series in terms of thickness co-ordinate. The governing equilibrium equation is obtained by using the principle of minimum potential energy and the solution for critical buckling load is obtained by solving the eigen value problem. The stability analysis of piezoelectric FG plate is carried out to present the effect of power law index and applied mechanical pressure. Results reveal that buckling strength increases with an increase in volume fraction. It can also be improved using piezo effects. The present analysis is carried out on newly introduced metal based FGM which is a mixture of aluminum and stainless steel which exhibits corrosion resistance as well as high strength property in a single material.
Keyword: functionally graded material, finite element method, piezoelectric material, FOST, HOST12, eigen value problem, electro-mechanical loading.

WIT Transactions on Modelling and Simulation, Vol 55,
www.witpress.com, ISSN 1743-355X (on-line)
doi:10.2495/CMEM130341

1 Introduction

Functionally graded materials are the microscopically inhomogeneous composite materials which exhibit smooth and continuous change of material properties along the thickness direction. Laminated composite structures face problems because of abrupt change in material properties and weakness of interfaces of layers placed between two adjacent laminates of composite structures. Such problems are overcome by using the FGM's. The advances in composite technology have lead to the increasing application of piezo laminated structure due to their sensing and actuating properties. Also, these structures have self-diagnostic and self-controlling capabilities. These structures can control the magnitude and mode of vibrations. Stability of the structural systems can also be enhanced because of their direct and converse piezoelectric effects.

Liew *et al.* [1] presented postbuckling behavior of piezoelectric FGM plate subject to thermo-electro-mechanical loading based on Reddy's higher-order shear deformation plate theory. Galerkin's differential quadrature iteration algorithm is proposed for solution of the non-linear partial differential governing equations. Shen [2] presented the postbuckling analysis for a simply supported, shear deformable functionally graded plate with piezoelectric actuators subjected to the combined action of mechanical, electrical and thermal loads. Shen [3] also presented the thermal postbuckling analysis for a simply supported shear deformable functionally graded plate under thermal loading]. The compressive postbuckling under thermal environments and thermal postbuckling due to a uniform temperature rise for a simply supported shear deformable functionally graded plate with piezoelectric fiber reinforced composite (PFRC) actuators has also been reported by Shen [4]. The above works done by Shen were based on higher order shear deformation plate theory and a two step perturbation technique was employed to determine buckling loads and postbuckling equilibrium paths. Chen *et al.* [5] used the element free Galerkin method to analyze buckling of piezoelectric FGM rectangular plates subjected to non-uniformly distributed loads, heat and voltage. Shariyat [6] developed finite element formulation based on a higher-order shear deformation theory to present the vibration and dynamic buckling of FGM rectangular plates with surface bonded piezoelectric sensors and actuators under the influence of thermo-electro-mechanical loading. A number of works have been carried out on stability analysis of smart FGM plate subjected to thermo-electro-mechanical loading.

To the best of the authors' knowledge, no work has been reported on the stability analysis of piezoelectric FGM plate subjected to electro-mechanical loading. This paper investigates the stability analysis of FG plate integrated with piezoelectric actuator and sensor at top and bottom face subjected to electro-mechanical coupling based on finite element method and considering FOST and HOST12, von-Karman hypothesis and degenerated shell element. Also this paper focuses to control the piezoelectric FGM plate against buckling by setting the optimum thickness of piezo layer. The present analysis is carried out on newly introduced metal based FGM material, which is a mixture of aluminum and

stainless steel. So this FGM exhibits the corrosion resistance and high strength property in single material.

2 Finite-element formulation

The figure 1 shows the general layout of FGM degenerated shell element integrated with piezoelectric actuator and sensor at top and bottom surface respectively. The figure 2 shows the geometry of eight noded isoparametric degenerated shell element [7]. For element geometry please refer to [10].

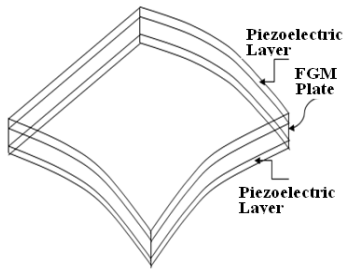

Figure 1: Piezoelectric FGM degenerated shell element.

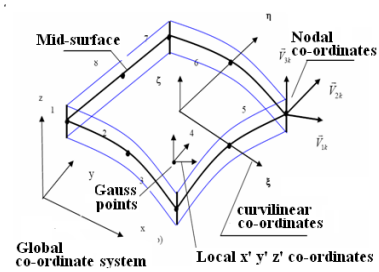

Figure 2: Geometry of an element.

The finite element formulation is based on eight noded degenerated element, FOST (First Order Shear Deformation Theory having five degrees of freedom per node) and HOST12 (Higher Order Shear Deformation Theory having twelve degrees of freedom per node) . The assumption made in the formulation of FOST (First Order Shear Deformation Theory) model is that the straight normal to the middle surface remain practically straight but not necessarily normal to mid surface during the deformation.

2.1 Element geometry and displacement field

In the isoparametric formulation co-ordinate of a point within the element are obtained as,

$$\begin{bmatrix} x \\ y \\ z \end{bmatrix} = \sum_{k=1}^{8} N_k \begin{bmatrix} x_k \\ y_k \\ z_k \end{bmatrix}_{mid} + \frac{\zeta}{2} \sum_{k=1}^{8} N_k \, t_k \begin{bmatrix} \hat{V}_{3k}^{x} \\ \hat{V}_{3k}^{y} \\ \hat{V}_{3k}^{z} \end{bmatrix} \tag{1}$$

where, $\hat{V}_{ik}^{j} \; (i = 1,2,3)$ is the j^{th} component of unit vector along nodal vector $\vec{V}_{ik}$ at node k and t_k is the thickness of shell at node k. x_k, y_k and z_k are the Cartesian coordinates of the midpoint of the shell at k^{th} node. The shape function N_k at k^{th} node is expressed as

$$N_k(\xi,\eta)=\frac{1}{4}(1+\xi\xi_k)(1+\eta\eta_k)(\xi\xi_k+\eta\eta_k-1) \qquad \text{for } k=1,2,3,4 \tag{2}$$

$$N_k(\xi,\eta)=\frac{1}{2}(1-\xi^2)(1+\eta\eta_k) \qquad \text{for } k=5,7 \tag{3}$$

$$N_k(\xi,\eta)=\frac{1}{2}(1+\xi\xi_k)(1-\eta) \qquad \text{for } k=6,8 \tag{4}$$

The displacement components of any point in the element are expanded in Taylor's series by using FOST and with the shear correction coefficient 5/6. The displacement component of any point within element in the global co-ordinate system in terms of thickness co-ordinate for FOST model [7], for HOST12 model as follows,

$$u_0(x,y,z)=u_0(x,y)+z\theta_x(x,y)+z^2u_0^*(x,y)+z^3\theta_x^*(x,y) \tag{5a}$$

$$v_0(x,y,z)=v_0(x,y)+z\theta_y(x,y)+z^2v_0^*(x,y)+z^3\theta_y^*(x,y) \tag{5b}$$

$$w_0(x,y,z)=w_0(x,y)+z\theta_z(x,y)+z^2w_0^*(x,y)+z^3\theta_z^*(x,y) \tag{5c}$$

Expressing the displacement field in a compact form

$$u=\sum_{k=1}^{n}[N]\{d^e\} \tag{6}$$

in which $[N]=[N1, N2, \ldots\ldots\ldots\ldots, N_n]$ is the shape function matrix for the entire element. $\{d^e\}=\{d_1^e, \ldots\ldots\ldots\ldots\ldots, d_n^e\}$ is the element displacement vector. The element displacement vector for the FOST (7) and HOST12 model, the element displacement vector is expressed as

$$\{d_k^e\}=\{u_m^k \quad v_m^k \quad w_m^k \quad \theta_x^k \quad \theta_y^k \quad \theta_z^k \quad u_m^{*k} \quad v_m^{*k} \quad w_m^{*k} \quad \theta_x^{*k} \quad \theta_y^{*k} \quad \theta_z^{*k}\}^T \tag{7}$$

where u_m^k, v_m^k and w_m^k are the displacement components of the midpoint of the normal in the global coordinate system. θ_x^k is a positive rotation of the normal about $\vec{V}_{1k}$, θ_y^k is a positive rotation about $\vec{V}_{2k}$ and θ_z^k is a positive rotation of the normal about $\vec{V}_{3k}$. The asterisk marked terms are higher order terms.

2.2 Strain displacement relation

In this formulation linear and nonlinear strains are expressed by using von Karman assumptions, the derivatives of the u' and v' with respect to x', y' and z' are small and their square terms are neglected, also neglecting the variation of w' with z'. The Green-Lagrange strains may be expressed in local co-ordinates as,

$$\{\varepsilon'\}=\begin{Bmatrix}\varepsilon_{x'}\\ \varepsilon_{y'}\\ \gamma_{x'y'}\\ \gamma_{x'z'}\\ \gamma_{y'z'}\end{Bmatrix}=\begin{Bmatrix}\partial u'/\partial x'\\ \partial v'/\partial y'\\ \dfrac{\partial u'}{\partial y'}+\dfrac{\partial v'}{\partial x'}\\ \dfrac{\partial u'}{\partial z'}+\dfrac{\partial w'}{\partial x'}\\ \dfrac{\partial v'}{\partial z'}+\dfrac{\partial w'}{\partial y'}\end{Bmatrix}+\begin{Bmatrix}\frac{1}{2}\left(\dfrac{\partial w'}{\partial x'}\right)^2\\ \frac{1}{2}\left(\dfrac{\partial w'}{\partial y'}\right)^2\\ \left(\dfrac{\partial w'}{\partial y'}\cdot\dfrac{\partial w'}{\partial x'}\right)\\ 0\\ 0\end{Bmatrix}=\{\varepsilon'^{L}\}+\{\varepsilon'^{NL}\}=\{\varepsilon'^{L}\}+\frac{1}{2}[S][G]\{d^e\} \tag{8}$$

where $\{\varepsilon'^{L}\}$ and $\{\varepsilon'^{NL}\}$ are the linear and nonlinear strain vectors respectively. $\varepsilon_{x'x'}$, $\varepsilon_{y'y'}$ and $\varepsilon_{z'z'}$ are the normal strains; $\gamma_{x'y'}$, $\gamma_{x'z'}$ and $\gamma_{y'z'}$ are the shear strains and u', v' and w' are the displacement components in the local co-ordinate system. These local derivatives are obtained from the global derivatives of the displacements u, v and w [7]. The displacement derivatives with respect to the ξ can be expressed for the FOST model [7] and for the HOST12 model as

$$\begin{Bmatrix}\dfrac{\partial u}{\partial \xi}\\ \dfrac{\partial v}{\partial \xi}\\ \dfrac{\partial w}{\partial \xi}\end{Bmatrix}=\sum_{k=1}^{n}N_{k,\xi}\begin{Bmatrix}u_0^k\\ v_0^k\\ w_{0i}^k\end{Bmatrix}+\sum_{k=1}^{n}N_{k,\xi}\,\zeta\frac{t_k}{2}\begin{bmatrix}-\hat{V}_{2k}^x & \hat{V}_{1k}^x & \hat{V}_{3k}^x\\ -\hat{V}_{2k}^y & \hat{V}_{1k}^y & \hat{V}_{3k}^y\\ -\hat{V}_{2k}^z & \hat{V}_{1k}^z & \hat{V}_{3k}^z\end{bmatrix}\begin{Bmatrix}\theta_x^k\\ \theta_y^k\\ \theta_z^k\end{Bmatrix}+$$
$$+\sum_{k=1}^{n}N_{k,\xi}\,\zeta\frac{t_k^2}{4}\begin{bmatrix}\hat{V}_{1k}^x & -\hat{V}_{2k}^x & \hat{V}_{3k}^x\\ \hat{V}_{1k}^y & -\hat{V}_{2k}^y & \hat{V}_{3k}^y\\ \hat{V}_{1k}^z & -\hat{V}_{2k}^z & \hat{V}_{3k}^z\end{bmatrix}\begin{Bmatrix}u_0^{*k}\\ v_0^{*k}\\ w_0^{*k}\end{Bmatrix}\quad+\sum_{k=1}^{n}N_{k,\xi}\,\zeta\frac{t_k^3}{8}\begin{bmatrix}-\hat{V}_{2k}^x & \hat{V}_{1k}^x & \hat{V}_{3k}^x\\ -\hat{V}_{2k}^y & \hat{V}_{1k}^y & \hat{V}_{3k}^y\\ -\hat{V}_{2k}^z & \hat{V}_{1k}^z & \hat{V}_{3k}^z\end{bmatrix}\begin{Bmatrix}\theta_x^{*k}\\ \theta_y^{*k}\\ \theta_z^{*k}\end{Bmatrix} \tag{9}$$

The derivatives with respect to η and ζ are obtained in a similar way.

1.1 Stress–strain relations

The stress–strain relation in the local co-ordinate system can be written as

$$\{\sigma\}=[C]\{\varepsilon\} \tag{10}$$

where, $\{\sigma\}=\begin{bmatrix}\sigma_{xx} & \sigma_{yy} & \sigma_{xy} & \sigma_{xz} & \sigma_{yz}\end{bmatrix}^T$ is the stress vector $\{\varepsilon\}$ is the strain vector and [C] is the elasticity matrix in global co-ordinates system. The [C] is obtained in global coordinates using the strain transformation matrix is given below [8]. The effective material properties for FGM plates by using power law function given as [9]

$$E_f=E_{m1}V_{m1}+E_{m2}V_{m2} \tag{11}$$

$$\text{But, } V_{m1}+V_{m2}=1 \text{ and } V_{m1}=\left(\frac{2z+h}{2h}\right)^n \tag{12}$$

$$E(z)=E_{m2}+(E_{m1}-E_{m2})\left(\frac{2z+h}{2h}\right)^n,\qquad \text{for} -h/2\le z\le h/2 \tag{13}$$

where E_{m1} and E_{m2} are the elastic moduli of aluminum and stainless steel respectively, V_{m1} and V_{m2} are the volume fraction of the aluminum and stainless steel respectively, n is power law index, z is thickness coordinate variable.

2.3 Electro-mechanical coupling

The linear piezoelectric constitutive equations coupling the elastic and electric fields can be respectively expressed as the direct and the converse piezoelectric equations are given as [10],

$$\{D\} = [e]\{\varepsilon\} + [g]\{E^p\} \tag{14}$$

$$\{\sigma\} = [C]\{\varepsilon\} - [e]^T\{E^p\} \tag{15}$$

where{D}is the electric displacement vector, [e] is the dielectric permittivity matrix, [g] is the dielectric matrix, [E] is the electric field vector, [σ] is the stress vector and [C] is the elastic matrix for a constant electric field.

2.4 Electrical potential function

One electrical degree of freedom is used per node for each sensor and actuator layers of an element. The electric field vector is assumed to be constant over an element of the piezoelectric layer and to vary linearly through the thickness of the piezoelectric layer. The electric field strength of an element in terms of the electrical potential of the actuator and sensor layers is expressed as

$$\{\mathbf{E}_a^p\} = -\sum_{i=1}^{n} \mathbf{B}_{a(i)}\, \phi_{a(i)}^e = -[\mathbf{B}_a]\{\phi_a^e\} = -\begin{bmatrix} 0 \\ 0 \\ 1/t_a \end{bmatrix}\{\phi_a^e\} \tag{16}$$

$$\{\mathbf{E}_s^p\} = -\sum_{i=1}^{n} \mathbf{B}_{s(i)}\, \phi_{s(i)}^e = -[\mathbf{B}_s]\{\phi_s^e\} = -\begin{bmatrix} 0 \\ 0 \\ 1/t_s \end{bmatrix}\{\phi_s^e\} \tag{17}$$

where t_a and t_s are the thickness of the actuator and sensor layers respectively, $\{\phi_a^e\}$ and $\{\phi_s^e\}$ are the nodal electric potential vectors for the actuator and sensor layers respectively and [B] is the field gradient matrix, can be given as follows

$$\{\phi_a^e\} = \{\phi_{a1}\ \phi_{a2}\ \phi_{a3} \ldots\ldots\ldots\ldots\ldots \phi_{an}\}^T, \quad n= 1, 2, 3, ..., 8 \tag{18}$$

$$\{\phi_s^e\} = \{\phi_{s1}\ \phi_{s2}\ \phi_{s3} \ldots\ldots\ldots\ldots\ldots \phi_{sn}\}^T, \quad n= 1, 2, 3, ..., 8 \tag{19}$$

2.5 Potential energy and stability criteria

Total potential energy is given by

$$\Pi^e = U^e - W^e \tag{20}$$

where U^e is the potential energy due to internal work done and W^e is the external work done by external forces. The internal potential energy U^e consisting of the

strain energy of the entire structure and the electrical potential energy of the piezoelectric layers can be written as

$$U^e = \frac{1}{2}\int_V \{\varepsilon^L\}^T \{\sigma\}\, dV - \frac{1}{2}\int_{V_a} \left[E_a^p\right]^T \{D_a\}\, dV - \frac{1}{2}\int_{V_s} \left[E_s^p\right]^T \{D_s\}\, dV + \int_V \{\varepsilon^N\}^T \{\sigma_0\} dV \quad (21)$$

where V, V_a, V_s and σ_0 are the volume of the entire structure, actuator layer, sensor layer and initial stress vector respectively. The work done by external forces due to the applied surface traction and applied electric charge on actuator is given as

$$W^e = \int_A \{d^e\}^T [N]^T \{\bar{\sigma}(x,y)\}\, dA + \int_{A_a} \{E_a\}^T \bar{q}_a(x,y)\, dA \quad (22)$$

where $\bar{\sigma}(x,y)$ and $\bar{q}_a^e(x,y)$ are the surface traction vector and specified surface charge density respectively. To minimize the total potential energy, the first variation of eqn. (20) is set to zero,

$$\delta\Pi^e = \delta U^e - \delta W^e = 0 \quad (23)$$

Substituting eqns (10), (14) and (15) in eqn. (21) and taking its first variation. Also taking the first variation of eqn. (22), resulting eqns (21) and (21) put in eqn. (32) and condensing the electrical degrees of freedom using static condensation the resulting equation can be written as

$$\left[K^e\right]\{d^e\} + \left[K_\sigma^e\right]\{d^e\} = \left[F_1^e\right] + \left[F_{ac}^e\right] \quad (24)$$

$$\left[K^e\right] = \left[K_d^e\right] + \left[K_{da}^e\right]\left[K_{aa}^e\right]^{-1}\left[K_{ad}^e\right] + \left[K_{ds}^e\right]\left[K_{ss}^e\right]^{-1}\left[K_{sd}^e\right] \quad (25)$$

$$\left[K_d^e\right]\{d^e\} + \left[K_{da}^e\right]\{\phi_a^e\} + \left[K_{ds}^e\right]\{\phi_s^e\} = \{F_1^e\} \quad (26)$$

$$\left[K_{ad}^e\right]\{d^e\} - \left[K_{aa}^e\right]\{\phi_a^e\} = \{Q_a^e\} \quad (27)$$

$$\left[K_{da}^e\right]\left[K_{aa}^e\right]^{-1}\{Q_a^e\} = \{F_{ac}^e\} \quad (28)$$

$$\left[K_{sd}^e\right]\{d^e\} - \left[K_{ss}^e\right]\{\phi_s^e\} = 0 \quad (29)$$

where the superscript e refers to the parameter at the element level and [K] matrices with subscripts d, da, ad, aa, ds and ss are defined below

$$\left[K_d^e\right] = \int_V [B]^T [C][B]\, dV \quad (30)$$

$$\left[K_{da}^e\right] = \left[K_{ad}^e\right]^T = \int_{Va} [B]^T [e][B_a]\, dV \quad (31)$$

$$\left[K_{aa}^e\right] = \int_{Va} [B_a]^T [g][B_a]\, dV \quad (32)$$

$$\left[K_{ds}^e\right] = \left[K_{sd}^e\right]^T = \int_{Vs} [B]^T [e][B_s]\, dV \quad (33)$$

$$\left[K_{ss}^e\right] = \int_{Vs} [B_s]^T [g][B_s]\, dV \quad (34)$$

$$\{F_1^e\} = \int_A [N]^T \{\bar{\sigma}(x, y)\} dA \tag{35}$$

$$\{Q_a^e\} = -\int_v [N_a]^T q_a^e dA \tag{36}$$

Assembling the element eqns (24), (26), (27) and (29) results in the global set of equations given as follows

$$[K]\{d\} + [K_\sigma]\{d\} = [F_1] + [F_{ac}] \tag{37}$$

$$[K_d]\{d\} + [K_{da}]\{\phi_a\} + [K_{ds}]\{\phi_s\} = \{F_1\} \tag{38}$$

$$[K_{ad}]\{d\} - [K_{aa}]\{\phi_a\} = \{Q_a\} \tag{39}$$

$$[K_{sd}]\{d\} - [K_{ss}]\{\phi_s\} = 0 \tag{40}$$

where $\{d\}$ is the global nodal generalized displacement vector, $\{\phi_a\}$ and $\{\phi_s\}$ are the global nodal generalized electric vector for the actuator and sensor layer respectively, eqn. (40) can be expressed as,

$$\{\phi_s\} = -[K_{ss}]^{-1}[K_{sd}]\{d\} \tag{41}$$

In case of constant gain velocity feedback control, the electrical potential to be fed back to the actuator $\{\phi_a\}$ is calculated as,

$$\{\phi_a\} = -G^* \{\phi_s\} \tag{42}$$

where $[G^*]$ is the feedback control gain matrix. In case of SISO (single input single output) system, the actuator and sensor voltage becomes a single value and control gain becomes a single value. The criteria for stability is obtained using the method of neutral equilibrium where the critical load is the load under which the structure can be in equilibrium both in the straight (initial) and the slightly bent configuration. $\lambda[K_\sigma]$ is geometric stiffness matrix based on an arbitrary reference intensity of membrane stresses. λ is a scalar multiplier which is determined such that, both the reference configuration represented by the load vector$\{d\}$and slightly deformed $\{\{d\}+\{\delta d\}\}$ remains in equilibrium configuration. $\{F_1\}$ and $\{F_{ac}\}$ are the mechanical force vectors and resulting force vector from applied charge on actuator layer.

$$([K] + \lambda[K_\sigma])\{d\} = \{F\} \tag{43}$$

$$([K] + \lambda[K_\sigma])(\{d\} + \{\delta d\}) = \{F\} \tag{44}$$

Subtracting eqn. (43) from eqn. (44) yields the Eigen value problem

$$([K] + \lambda[K_\sigma])\{\delta d\} = 0 \tag{45}$$

where the critical buckling load is associated with the lowest magnitude eigen value and the displacement vector **{**$\delta d\}$ represents the buckled mode shape.

3 Numerical results and discussion

Example 1: Stability analysis of FGM plate having size 1.2 m x 1.2 m and 0.06m thickness is done. FGM plate is mixture of aluminum and stainless steel with piezoelectric actuator and sensor at top and bottom with thickness of piezoelectric actuator (t_a) and sensor (t_s) is 0.0025 m. Plate is simply supported at all edges (SSSS) and it is subjected to uniaxial compressions (figure 4). The elastic modulus of aluminum and stainless steel is 70 Gpa and 193 Gpa respectively, Poisson's ratio is 0.3, piezostrain constants (e31, e32) is 0.046 C/m^2 and Electric permittivity (ε11) is 1.060e-10 F/m [10]. As per analytical method (11), critical buckling load is expressed as, $N_{cr} = K_{cr}\,\Pi^2 D/b^2$ in which b is the width of plate, D is the rigidity modulus of plate (i.e. $D = Eh^3/[12(1-\upsilon^2)]$ with E, the Young's modulus) and K_{cr}=4 for isotropic plate. Present analysis calculate the critical buckling load by solving eigen value problem gives $N_{cr}=\lambda * N_x$ in which N_x is applied load and λ is the lowest magnitude of eigen value. Since there are no appropriate comparison results available for the FGM with the mixture of aluminum and stainless steel, so comparison of results are made with analytical results [11], ANSYS nonlinear analysis results for n=0 i.e. isotropic plate and FOST results. The results are presented for critical buckling load (N_{cr}) for various volume fraction indices thorough the thickness as 0, 3, 5, 7, 9, and 10. As per analytical method critical buckling load is calculated as 1.05E8 N/m for simply supported isotropic stainless steel plate subjected to uniaxial compression [11], nonlinear ANSYS finite element analysis gives critical buckling load is 1.14E8 N/m for simply supported isotropic stainless steel plate subjected to uniaxial compression (figure 5).

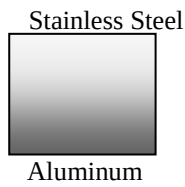

Figure 3: FGM plate with variation of material.

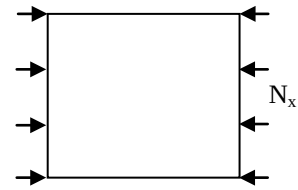

Figure 4: Plate subjected to uniaxial compression.

Tables 1 and 2 show the critical buckling load of FGM plate using HOST model without and with piezo effect and Tables 3 and 4 show the critical buckling load of FGM plate using FOST model without and with piezo effect. The critical buckling load obtained by applying 1.2E+08 N/m axial compression to FGM plate without piezo effect (In case of FGM n=0 is assumed to be an isotropic plate) are 9.951E+07N/m and 9.824E+07 N/m for HOST and FOST model respectively. The HOST results are closely agreed with and FOST results also results are closely agreed with analytical results and ANSYS nonlinear program results. The buckling strength of FGM plate can be improved by using

piezo layers and the improved buckling loads for HOST model is (i.e. n=0) 1.101E+08N/m and for FOST model is 1.077E+08 N/m with gain of 5 and 3.9 respectively.

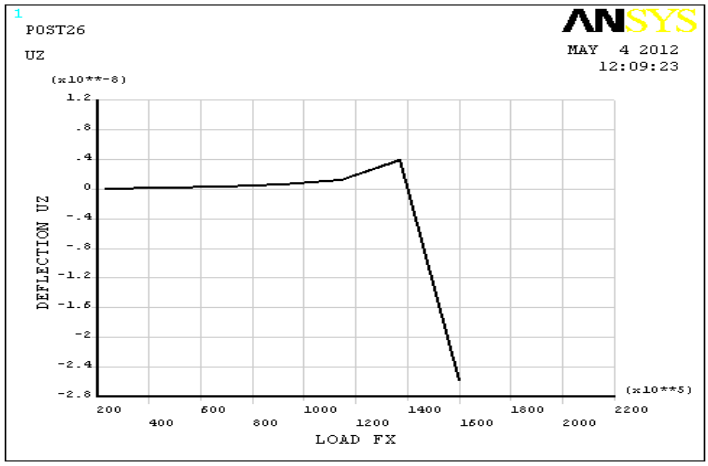

Figure 5: Buckling load of isotropic steel plate without piezo effect.

Table 1: Buckling load (N_{cr}) of simply supported Al/SUS304 plate under uniaxial compression without piezo effect (HOST12, t_a= t_s=0.0025) x1E+07 (N/m x1E7).

z/h	Load	n=0	n=3	n=5	n=7	n=9	n=10
0.5	12	9.951	9.951	9.951	9.951	9.951	9.951
0		9.951	4.151	4.303	4.085	5.335	5.989
-0.5		9.951	3.696	3.696	3.696	3.696	3.696

Table 2: Buckling load (N_{cr}) of simply supported Al/SUS304 plate under uniaxial compression with piezo effect (HOST12, t_a= t_s=0.0025) (N/m x1E7).

z/h	Load	Gain	n=0	n=3	n=5	n=7	n=9	n=10
0.5	12	5.0	11.01	11.01	11.01	11.01	11.01	11.01
0			11.01	4.804	5.061	5.304	6.077	6.282
-0.5			11.01	4.154	4.154	4.154	4.154	4.154

Table 3: Buckling load (N_{cr}) of simply supported Al/SUS304 plate under uniaxial compression without piezo effect (FOST, t_a= t_s=0.0025) (N/m x1E7).

z/h	Load	n=0	n=3	n=5	n=7	n=9	n=10
0.5	12	9.824	9.824	9.824	9.824	9.824	9.824
0		9.824	3.876	4.285	4.751	5.206	5.818
-0.5		9.824	3.523	3.523	3.523	3.523	3.523

Table 4: Buckling load (N_{cr}) of simply supported Al/SUS304 plate under uniaxial compression with piezo effect (FOST, t_a= t_s=0.0025) (N/m x1E7).

z/h	Load	Gain	n=0	n=3	n=5	n=7	n=9	n=10
0.5	12	3.9	10.77	10.77	10.77	10.77	10.77	10.77
0			10.77	4.708	5.038	5.247	5.785	6.148
-0.5			10.77	3.999	3.999	3.999	3.999	3.999

Example 2: Solving above problem for stability analysis of piezoelectric FGM plate by changing the thickness of piezoelectric actuator (t_a) and sensor (t_s) is 0.004 m for the purpose of buckling control of thick FGM plate easily.

Tables 5 and 6 show the critical buckling load of FGM plate using HOST model without and with piezo effect and Tables 7 and 8 show the critical buckling load of FGM plate using FOST model without and with piezo effect. The critical buckling load obtained by applying 1.2E+08 N/m axial compression to FGM plate without piezo effect (In case of FGM n=0 is assumed to be an isotropic plate) are 1.011E+08 N/m and 1.004E+08 N/m for HOST and FOST respectively. The buckling strength of FGM plate can be improved by using piezo layers and improved buckling loads for HOST model is (i.e. n=0) 1.238E+08 N/m and for FOST model is 1.152E+08 N/m with gain of 5 and 3.9 respectively.

Table 5: Buckling load (N_{cr}) of simply supported Al/SUS304 plate under uniaxial compression without piezo effect (HOST12, t_a= t_s=0.004) (N/m x1E7).

z/h	Load	n=0	n=3	n=5	n=7	n=9	n=10
0.5	12	10.11	10.11	10.11	10.11	10.11	10.11
0		10.11	4.411	4.549	5.307	5.859	6.174
-0.5		10.11	3.891	3.891	3.891	3.891	3.891

Table 6: Buckling load (N_{cr}) of simply supported Al/SUS304 plate under uniaxial compression with piezo effect (HOST12, t_a= t_s=0.004) (N/m x1E7).

z/h	Load	Gain	n=0	n=3	n=5	n=7	n=9	n=10
0.5	12	11.0	12.38	12.38	12.38	12.38	12.38	12.38
0			12.38	4.795	4.946	5.691	5.938	6.442
-0.5			12.38	4.026	4.026	4.026	4.026	4.026

Table 7: Buckling load (N_{cr}) of simply supported Al/SUS304 plate under uniaxial compression without piezo effect (FOST, t_a= t_s=0.004) (N/m x1E7).

z/h	Load	n=0	n=3	n=5	n=7	n=9	n=10
0.5	12	10.04	10.04	10.04	10.04	10.04	10.04
0		10.04	4.151	4.341	5.042	5.54	5.943
-0.5		10.04	3.8	3.8	3.8	3.8	3.8

Table 8: Buckling load (N_{cr}) of simply supported Al/SUS304 plate under uniaxial compression with piezo effect (FOST, t_a= t_s=0.004) (N/m x1E7).

z/h	Load	Gain	n=0	n=3	n=5	n=7	n=9	n=10
0.5	12	4.0	11.52	11.52	11.52	11.52	11.52	11.52
0			11.52	4.66	4.782	5.142	5.713	6.062
-0.5			11.52	3.778	3.778	3.778	3.778	3.778

The overall result shows that the buckling of plate can be controlled by using piezoelectric layer and present analysis gives good agreement of controlled buckling load of FGM plate with piezo thickness of 0.004m as compared with results of plate with piezo thickness of 0.0025m. Overall result shows that buckling strength of plate goes on increasing with increase in volume fraction indices through the thickness. Also the strength of plate increases from bottom to top of FGM plate i.e. from aluminum to steel. The HOST results are closely agreed with and FOST results also results are closely agreed with analytical results and ANSYS nonlinear program results.

4 Conclusion

The finite element model for stability analysis of piezo laminated FGM plate using HOST12 and FOST is developed. One electrical degree of freedom per element is used in the formulation. The equation for static analysis is derived using the minimum energy principle. The validation for the stability analysis is performed by comparing the buckling load results of FGM plate without and with piezo-electric effect using the analytical results, ANSYS nonlinear finite element analysis results of isotropic stainless steel plate (n=0) and FOST model results for FGM plate with different piezo layer thickness.

Numerical studies on piezoelectric thick FGM plate for stability analysis using SISO control strategy suggested that buckling of FGM plate can be controlled by increasing the gain values. The buckling analysis is performed for different values of gains for different loading conditions as well as piezo thickness. Present analysis predicts that buckling strength of plate can be improved by using higher piezo layer thickness easily as compare to the lower piezo thickness. Overall results show that, buckling strength of plate increases with the increase in volume fraction indices through the thickness. Also the piezo thickness significantly influences the buckling control of plate with different gain values. The difference between HOST12 and FOST mode results are less and closely agree with the results of ANSYS nonlinear finite element analysis of isotropic stainless steel plate.

References

[1] Liew, K.M., Yang, J. and Kitipornchai, S. Postbuckling of piezoelectric FGM plates subject to thermo-electro-mechanical loading. *International Journal of Solids and Structures*, **40,** pp. 3869-3892, 2003.

[2] Shen, H.S. Postbuckling of FGM plates with piezoelectric actuators under thermo-electro-mechanical loadings. *International Journal of Solids and Structures*, **42,** pp. 6101-6121, 2005.

[3] Shen, H.S. Thermal postbuckling behavior of shear deformable FGM plates with temperature-dependent properties. *International Journal of Mechanical Sciences*, **49,** pp. 466-478, 2007.

[4] Shen, H.S. A comparison of buckling and postbuckling behavior of FGM plates with piezoelectric fiber reinforced composite actuators. *Composite Structures*, **91,** pp. 375-384, 2009.

[5] Chen, X.L., Zhao, Z.Y. and Liew, K.M. Stability of piezoelectric FGM rectangular plates subjected to non-uniformly distributed load, heat and voltage. *Advances in Engineering Software*, **39,** pp. 121-131, 2008.

[6] Shariyat, M. Vibration and dynamic buckling control of imperfect hybrid FGM plates with temperature-dependent material properties subjected to thermo-electro-mechanical loading conditions. *Composite Structures*, **88,** pp. 240-252, 2009.

[7] Jadhav, P. and Bajoria, K. Stability Analysis of Functionally Graded Plate Integrated with Piezoelectric Actuator and Sensor Subjected to Electro-Mechanical Loading. *Proc. of the 4th International Conference on Structural Stability and Dynamic*, MNIT Jaipur, India, vol.-II, pp. 647-56, 2012.

[8] Bathe, K.J. *Finite element procedures*, 2nd edn. (Englewood Cliffs, NJ, Prentice-Hall), 1996.

[9] Javaheri, R. and Eslami, M.R., Buckling of functionally graded plates under in-plane compressive loading. *Journal of Applied Mathematics and Mechanics*, **82**, pp. 277-283, 2000.

[10] Kulkarni, S.A. and Bajoria, K.M., Finite element modeling for the smart plates/shells using higher order theory. *Composite Structures*, **62,** pp. 61-50, 2003.

[11] Timoshenko, S. *Theory of elastic stability. Tata McGraw-Hill Education*, pp. 327-332.

[12] Jadhav, P. and Bajoria, K. Stability Analysis of Functionally Graded Plate Integrated with Piezoelectric Actuator and Sensor Subjected to Electro-Mechanical Loading. *International Journal of Structural Stability and Dynamics* (Communicated).